LenteraBio, 2025; Volume 14, Issue 2: 219-228

p-ISSN: 2252-3979 e-ISSN: 2685-7871
https://journal.unesa.ac.id/index.php/lenterabio/index

Effect of Polystyrene Nanoplastic on Colon, Liver, and Spleen Histopathology of Rats (*Rattus norvegicus* L.)

Diyah Utari[1], Alfiah Hayati[1*], Inge Permatasari[1], Lina Afiifatul Abroroh[1], Nisrina Qatrunada[1], Rosida[1], Sasanaqia Maulidah[1], Mardhiah Hayati[1], Putri Ayu Ika Setiyowati[1], Dwi Winarni[1], Sugiharto[1], Firli Rahmah Primula Dewi[1], Manikya Pramudya[1]

[1]Department of Biology, Faculty of Science and Technology, Universitas Airlangga, Surabaya.
[2]Department of Biology, Faculty of Science and Data Analytics, Institut Teknologi Sepuluh Nopember, Surabaya
[*)] Corresponding author: alfiah-h@fst.unair.ac.id

Article History:
Received:
2-June-2025
Revised:
21-May-2025
Available online:
31-May-2025
Published regularly:
31-May-2025

Abstract

Polystyrene, when exposed to ultraviolet light, can break down into nanoplastics (NPs), which enter the body and elevate reactive oxygen species, leading to oxidative stress which can damage cell structure and function by causing inflammation, necrosis, and tissue degeneration in target organs such as the colon, liver, and spleen. This study specifically investigates the impact of NPs on rats' colons, livers, and spleens. The experimental design was completely randomized, comprising one control group and three treatment groups (n=6). The treatment groups were exposed to NPs concentrations of 1, 2, and 4 µL/kg, administered orally for 35 days. Tissue samples from the colon, liver, and spleen were collected, processed, and stained with H&E. Findings in the colon indicated an increase in submucosal and muscular thickness and a reduction in crypt length with higher NPs concentrations. In the liver, higher NPs concentrations resulted in a decrease in the percentage of normal and oedematous hepatocytes, along with an increase in necrotic hepatocytes, Kupffer cells, and the diameters of the portal and central veins. The spleen showed enlargement in the white pulp and germinal centre diameters, and increased thickness in the periarterial lymphoid sheath (PALS) and marginal zone. This study highlights the critical need to reduce NPs pollution to mitigate potential health risks.

Keywords: colon; health; hepatocytes; nanoplastics; spleen

How to Cite: Utari D, Permatasari I, Abroroh LA, Qatrunada N, Rosida R, Maulidah S, Hayati M, Setiyowati PAI, Winarni D, Sugiharto S, Dewi FRP, Pramudya M, Hayati A, 2025. Effect of Polystyrene Nanoplastic on Colon, Liver, and Spleen Histopathology of Rats (*Rattus norvegicus* L.). LenteraBio; Volume 14(2): 219-228

DOI: https://doi.org/10.26740/lenterabio.v14n2.p219-228

INTRODUCTION

Plastic is a polymer compound widely used by humans to simplify various tasks. According to Indonesia's Ministry of Environment and Forestry, the country's waste production in 2022 reached 18,893,843.32 tons per year, with plastic waste accounting for 18,764 tons or 18.2%, making it the second most prevalent type of waste after food waste. Although not the largest contributor, plastic waste is challenging to decompose and requires a long degradation period, necessitating specialized treatment (Kibria *et al.,* 2023). Commonly used plastics include polyethylene (PE), polypropylene, polystyrene (PS), and terephthalate (Clarinsa and Sutoyo, 2021). Among these, polystyrene stands out, with an annual usage exceeding 23 million tons (Lithner *et al.,* 2011). Polystyrene is considered hazardous due to its high surface area, allowing it to easily penetrate cell membranes and potentially disrupt cell functions (Phuong *et al.,* 2016; Hayati *et al.,* 2022a).

Over time, plastic degrades into microplastic particles, which can further break down into NPs under prolonged ultraviolet exposure (Hayati, 2022b). Microplastics vary in size, ranging from 1–5 mm (large) to smaller particles (<1 mm), while NPs measure less than 0.1 µm (Tankovic *et al.,* 2015). NPs can enter the body via three primary pathways: inhalation (e.g., from paint), dermal absorption (e.g., from cosmetics), and ingestion (e.g., through food and drink). Once accumulated, these particles can induce oxidative stress (Hayati *et al.,* 2024; Triwahyudi *et al.,* 2023), a condition marked by increased oxidants or Reactive Oxygen Species (ROS) and reduced antioxidants (Pizzino *et al.,* 2017; Hayati, 2022b). Excess

ROS can damage cell membranes, disrupting metabolic and bodily functions. NPs significantly impact organs such as the liver, spleen, and colon. Ingested particles can penetrate the colonic barrier and spread to other tissues, as seen in studies where NPs were detected in the stomach, colon, and liver of rodents (Soepriandono *et al.,* 2025).

The colon plays a critical role in water and electrolyte absorption, vitamin production and absorption, and fecal formation (Giri *et al.,* 2021). The liver, essential for metabolism, detoxification, and conjugation, is highly susceptible to damage (Yin *et al.,* 2022). Meanwhile, the spleen, located in the upper left abdomen, is vital for immune function as it produces white blood cells, including lymphocytes (Lewis *et al.,* 2019).

Damage caused by NPs to cell membranes in these organs disrupts their stability, leading to metabolic irregularities and changes in osmotic pressure. Such instability can result in cell swelling, abnormalities, or death. Despite the significant health risks posed by NPs, research on their effects, particularly in Indonesia, remains limited. Therefore, studying the impact of NPs exposure on organ histology, specifically in the colon, liver, and spleen using rat models, is essential to better understand their adverse effects.

MATERIALS AND METHODS

The study used 24 male Wistar rats (*Rattus norvegicus L.*), aged 6–8 weeks and weighing 100–150 grams. The NPs solution (Sigma Aldrich NIST1963A) had a particle size of 100 nm. Three treatment doses were prepared: Treatment 1-3 (P1-P3) used 1, 2, and 4 µL kg. Each treatment group received 0.5 mL of solution. For example, in P1, 0.5 mL consisted of 0.001 mL NPs and 0.499 mL distilled water, resulting in a stock solution of 17.5 mL for 35 days (0.035 mL NPs mixed with 17.465 mL distilled water). The same method was applied for P2 and P3, adjusting the NP doses accordingly.

Rats were acclimated for two weeks in laboratory conditions, provided with pellets and distilled water ad libitum, and housed in plastic containers lined with wood husks. NPs solutions (0.5 mL) were administered orally for 35 days between 15:00 and 17:00 WIB. On the 36th day, rats were anesthetized using chloroform, dissected, and their colon, liver, and spleen were extracted. These organs were preserved in a neutral buffer formalin (NBF) fixative solution within urine containers.

The organs (colon, liver, and spleen) were prepared using the paraffin method. The process began with fixation in NBF solution, followed by washing and cutting the tissues placed into embedding cassettes and soaked in running water overnight. The tissues underwent dehydration, clearing, infiltration, and embedding in paraffin blocks. Sectioning was performed using a microtome to create slices approximately 4 µm thick, which were floated on a 40°C water bath and mounted on glass slides coated with Mayer's albumin, then incubated overnight. Staining was performed using Hematoxylin and Eosin dyes, followed by mounting with Entellan adhesive between the slide and cover glass. The prepared histological slides of the colon, liver, and spleen were observed under a binocular light microscope equipped with an Optilab camera. Liver samples were analyzed to evaluate hepatocytes (normal, edematous, necrotizing), Kupffer cells, and the diameters of the portal and central veins using a calibrated micrometer. Colon samples were examined to measure submucosa thickness, muscularis thickness, and crypt length using Optilab Viewer 4 software. Spleen samples were analyzed using a microscope to measure the white pulp diameter, germinal center diameter, PALS thickness, and marginal zone thickness.

Statistical analysis was performed using IBM SPSS version 25. Normality was assessed with the One-Sample Kolmogorov-Smirnov test ($\alpha > 0.05$). Normally distributed data were analyzed using One-Way ANOVA with a significance level of 0.05, followed by Duncan's Post Hoc test to identify differences between groups. Non-normally distributed data were analyzed using the Kruskal-Wallis test with a significance level of 0.05, followed by the Mann-Whitney U test for pairwise comparisons.

RESULTS

The colon's histological parameters analyzed included the width of the muscularis, the width of the submucosa, and the length of the crypts. Observations revealed that as the concentration of NPs increased, both the muscularis and submucosa widths expanded, as indicated by the upward trend in the graph (Figures 1 and 2). Conversely, the crypt length exhibited a decreasing trend with higher NPs concentrations. The average values for each parameter are presented in Table 1.

Table 1. Observation parameter of histology on the colon of the rat

Parameter	Treatment Group with NPs			
	0 µL/kg	1 µL/kg	2 µL/kg	4 µL/kg
Submucosal Width (µm)	30.94 ± 0.35[a]	45.01 ± 0.78[b]	52.81 ± 0.50[c]	77.77 ± 0.38[d]
Muscular Width (µm)	91.81 ± 1.32[a]	146.06 ± 0.66[b]	174.59 ± 0.77[c]	205.16 ± 0.88[d]
Crypt Length (µm)	283.79 ± 0.70[d]	227.31 ± 0.58[c]	218.48 ± 1.65[b]	207.08 ± 0.47[a]

Notes: Different superscript letters behind the numbers in the same row indicate significant differences (P<0.05).

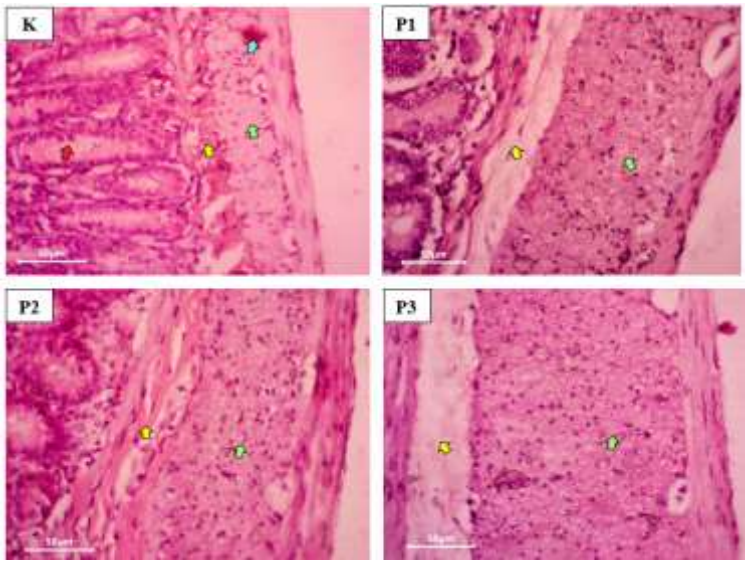

Figure 1. Histopathology of submucosa and muscularis of rat colon at various concentrations of NPs. K = Sterile distilled water, P1 = 1 µL/kg NPs, P2 = 2 µL/kg NPs, P3 = 4 µL/kg NPs. Blue arrow: hemorrhage, green arrow: muscularis, yellow arrow: submucosa, red arrow: crypts.

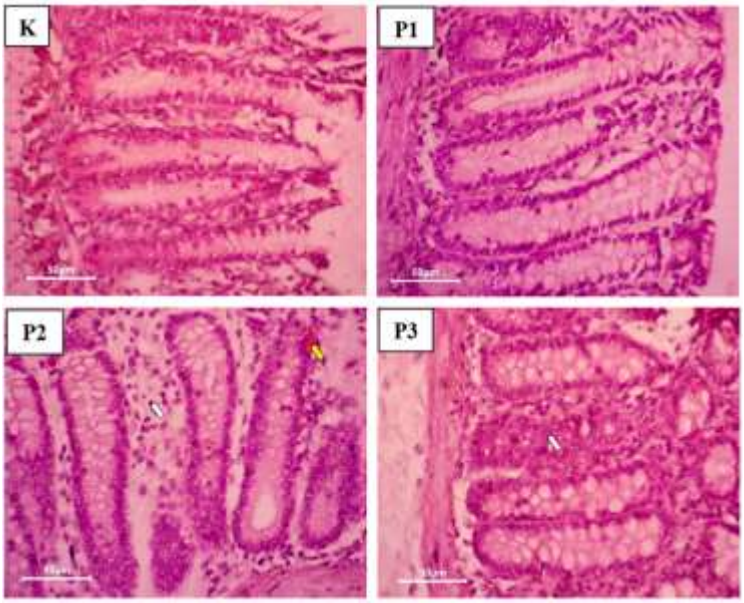

Figure 2. Histopathology of rat colon crypts at various concentrations of NPs. K = Sterile distilled water, P1 = 1 µL/kg NPs, P2 = 2 µL/kg NPs, P3 = 4 µL/kg NPs. Yellow arrow: hemorrhage, white arrow: leukocyte infiltration.

The liver histology analysis included parameters such as the number of normal hepatocytes, edema, necrosis, Kupffer cells, and the diameters of the portal and central veins. The number of normal hepatocytes decreased with increasing doses of NPs. Edema showed an initial increase at a dose of 1.0 µL NPs/kg but decreased with higher doses. In contrast, necrosis and Kupffer cells increased with higher NPs doses. The portal and central vein diameters displayed the greatest dilation at a dose of 1.0 µL NPs/kg. Detailed average values for these parameters are provided in Table 2.

Table 2. Observation results and parameter calculations on liver histology

Parameters	Treatments Group with NPs			
	0 µL/kg	1 µL/kg	2 µL/kg	4 µL/kg
Normal Hepatocytes (%)	84.84 ± 1.2[a]	63.45 ± 2.63[b]	52.52 ± 2.87[c]	47.85 ± 1.67[d]
Edema Hepatocytes (%)	2.97 ± 0.24[a]	19.14 ± 1.52[b]	17.57 ± 1.68[c]	8.85 ± 1.38[c]
Hepatocytes Necrosis (%)	12.18 ± 1.22[a]	17.04 ± 2.00[b]	29.91 ± 2.72[c]	43.31 ± 2.31[d]
Kupffer Cells (number)	12.18 ± 1.23[a]	42 ± 1.57[b]	64 ± 4.82[c]	104 ± 6.62[c]
Portal Vein Diameter (µm)	12.18 ± 1.24[a]	69.94 ± 3.15[a]	74.43 ± 2.44[b]	132.44 ± 5.62[c]
Central Vein Diameter (µm)	12.18 ± 1.25[a]	51.49 ± 4.24[ab]	58.04 ± 5.81[b]	76.64 ± 7.48[c]

Notes: Different superscript letters behind the numbers in the same row indicate significant differences (P<0.05).

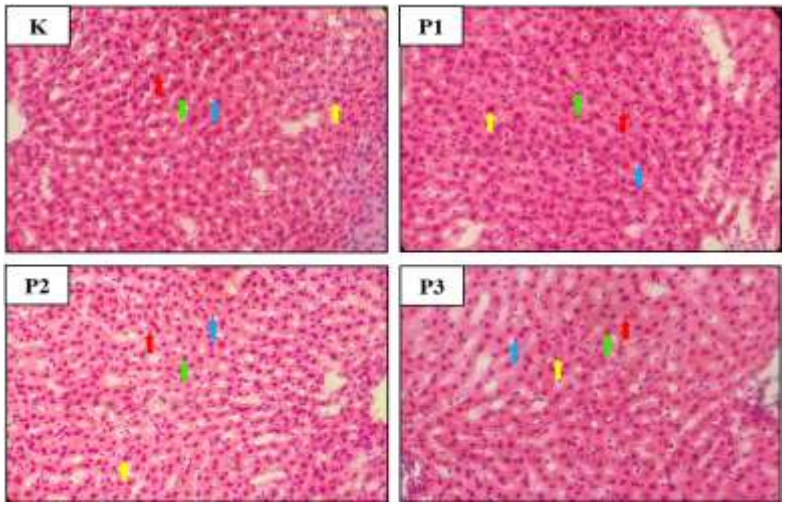

Figure 3. Histopathological analysis of rat liver given different NPs concentrations. K = Sterile distilled water, P1 = 1 µL/kg NPs, P2 = 2 µL/kg NPs, P3 = 4 µL/kg NPs. Green arrow: normal hepatocytes, yellow arrow: hepatocytes with edema, red arrow: necrotic hepatocytes, blue arrow: Kupffer cells.

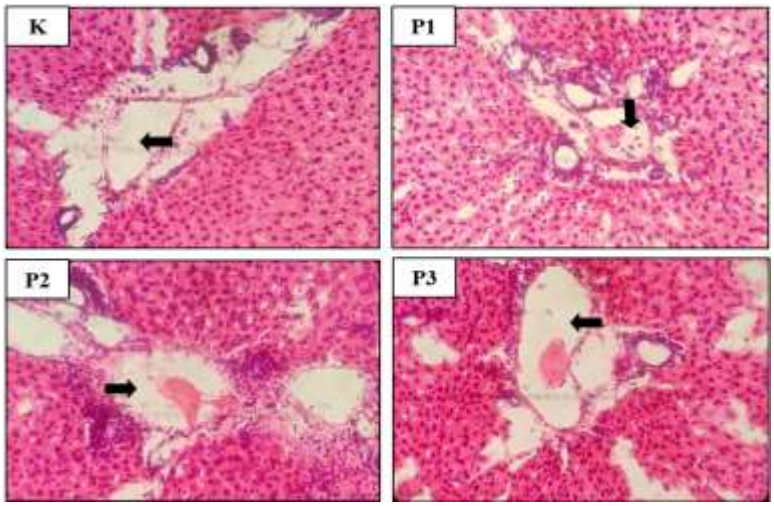

Figure 4. Histopathological examination of the portal vein in the rat liver given various concentrations of NPs. K = Sterile distilled water, P1 = 1 µL/kg NPs, P2 = 2 µL/kg NPs, P3 = 4 µL/kg NPs. Black arrow: portal vein.

Evaluation showed that the diameter of the white pulp, germinal center, PALS thickness, and marginal zone thickness increased progressively with higher doses of NPs (Figure 6). The smallest values for all parameters were observed in the control group, while a dose of 1 µL/kg NPs resulted in a noticeable increase. This upward trend persisted with escalating doses, with the highest measurements recorded at 4 µL/kg NPs. Detailed data for these changes are presented in Table 3.

Table 3. Observation results and parameter calculations on spleen histology

Parameters	Treatments Group with NPs			
	0 µL/kg	1 µL/kg	2 µL/kg	4 µL/kg
Normal Hepatocytes (%)	635.74 ± 3.93[a]	752.95 ± 2.40[b]	833.56 ± 3.12[c]	1015.20 ± 6.18[d]
Edema Hepatocytes (%)	125.02 ± 3.51[a]	162.42 ± 2.67[b]	193.70 ± 3.27[c]	222.07 ± 3.02[d]

Hepatocytes Necrosis (%)	64.56 ± 3.13[a]	74.53 ± 1.65[b]	81.48 ± 1.47[c]	86.77 ± 1.58[d]
Kupffer Cells (number)	55.48 ± 1.73[a]	63.87 ± 1.70[b]	68.53 ± 0.90[c]	75.02 ± 1.21[d]

Notes: Different superscript letters behind the numbers in the same row indicate significant differences (P<0.05).

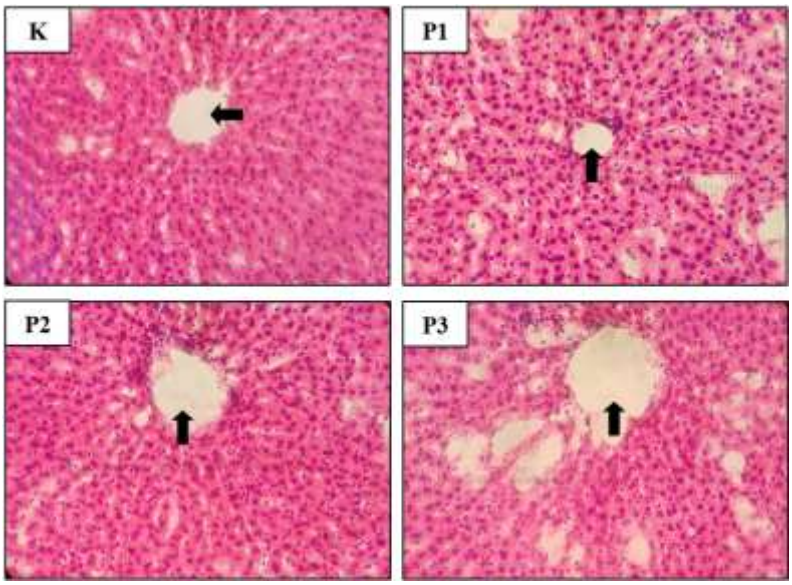

Figure 5. Histopathological analysis of the central vein in the rat liver given different concentrations of NPs. K = Sterile distilled water, P1 = 1 µL/kg NPs, P2 = 2 µL/kg NPs, P3 = 4 µL/kg NPs. Black arrow: central vein.

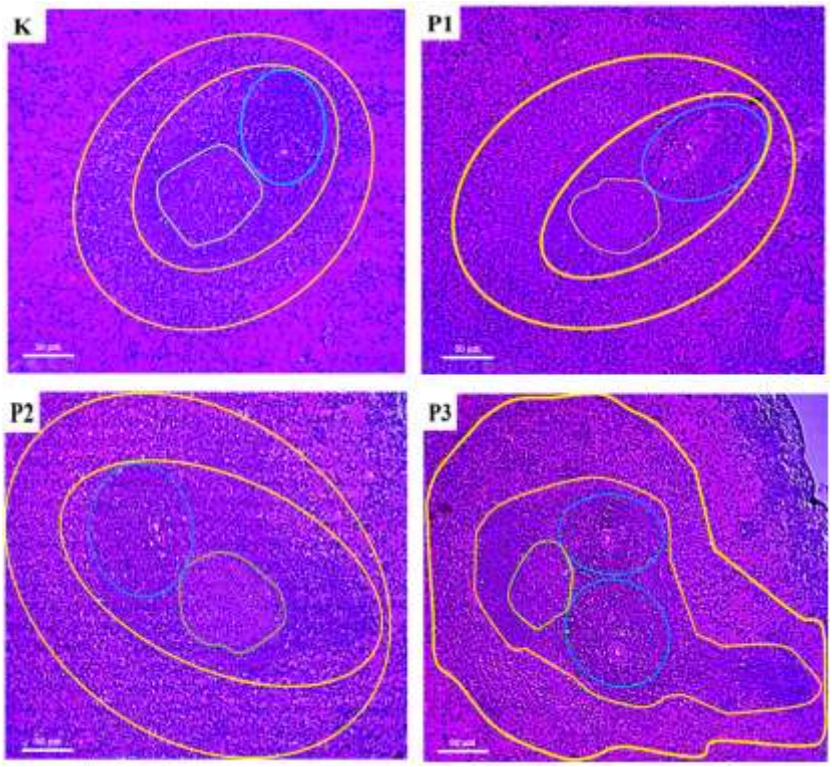

Figure 6. Histopathological examination of the rat spleen given different NPs concentrations. K = Sterile distilled water, P1 = 1 µL/kg NPs, P2 = 2 µL/kg NPs, P3 = 4 µL/kg NPs. The yellow circular line indicates the border of the white pulp and marginal zone, the blue circular line marks the PALS, and the green circular line outlines the germinal centre.

DISCUSSION

Plastic is a polymer made up of repeating monomers that form chains. In this study, polystyrene, a synthetic plastic known for its high surface area and ability to easily penetrate cell membranes, was used. These characteristics can disrupt cell function (Liu *et al*., 2016; Phuong *et al*., 2016). Plastic waste can degrade into smaller particles such as microplastics (<1 mm) and NPs (<0.1 µm)

through physical, chemical, and biological processes (Kwak & An, 2021; Tankovic *et al.,* 2015). Due to their small size, NPs particles possess a large surface area and high ability to absorb contaminants, resulting in increased toxicity (Liu *et al.,* 2016; Joksimovic *et al.,* 2022). When NPs enter the body via endocytosis, they can increase the production of Reactive Oxygen Species (ROS). The accumulation of ROS and the distribution of NPs through blood vessels can lead to oxidative stress, which damages cellular structures, affecting body functions and metabolism.

Exposure to NPs showed significant histopathological effects on the rat colon in a dose-dependent manner, with obvious structural changes in the colon tissue layers. Based on the quantitative data in Table 1, increasing the dose of NPs led to an increase in the thickness of the submucosa and muscularis layers, as well as a decrease in the length of the colonic crypts, indicating an inflammatory response and tissue damage. This increase in the thickness of the submucosa and muscularis layers may reflect the occurrence of oedema, cell proliferation, and inflammation as the body's reaction to toxic stressors. These findings are in line with the study of Lim et al. (2021), which reported that NPs can activate inflammatory pathways and increase the formation of pro-inflammatory cytokines, which play a role in gastrointestinal tissue thickening. In Figure 1, the colon tissue structure of the control group (K) looks normal and regular, but in groups P1 to P3 exposed to NPs, there was obvious thickening in the submucosa (yellow arrow) and muscularis (green arrow) layers, accompanied by haemorrhagic areas (blue arrow). The higher the dose of NPs administered, the more pronounced these changes were, reflecting chronic inflammation. This is consistent with the results shown in Table 1, which showed a significant dose-response relationship in the thickness of the tissue layer.

Figure 2 shows significant changes in the structure of the colonic crypts. In the control group (K), the colonic crypts showed a regular and elongated shape, with little leukocyte infiltration. However, in groups P1 to P3, the crypts were degenerated, with a reduction in length and increased leukocyte infiltration (white arrows), as well as haemorrhage (yellow arrows). This apparent decrease in crypt length, which is consistent with the quantitative data in Table 1, indicates impaired differentiation and proliferation of epithelial cells, which is indicative of impaired homeostasis of the intestinal epithelium. These findings support the study by Yong et al. (2020), which revealed that NPs exposure can interfere with intestinal epithelial regeneration through increased oxidative stress and disruption of the Wnt/β-catenin pathway, which is essential for crypt differentiation and regeneration.

Leukocyte infiltration also indicates the activation of the local immune system in response to tissue damage, where immune cells move to the damaged area. Although this is part of the body's defense response, in chronic exposure, it can worsen tissue damage, as stated by Jin et al. (2022), who stated that the accumulation of NPs in colonic tissue can stimulate the expression of TNF-α and IL-6, exacerbating local inflammation. Detected tissue bleeding (haemorrhage) is also an indicator of blood vessel damage, which may be caused by oxidative stress or extracellular matrix degradation. As reported by Wu et al. (2019), NPs can damage tight junctions between epithelial cells, increasing abnormal intestinal permeability and allowing fluid and blood cell leakage into the tissue. Overall, the combination of evidence from microscopic observations (Figures 1 and 2) and quantitative results (Table 1) suggests that polystyrene NPs exposure causes damage to colonic tissue structure in a dose-responsive manner, with the main mechanisms involved being inflammatory activation, oxidative stress, immune cell infiltration, and impaired epithelial regeneration. This indicates the potential risk of NPs toxicity to the gastrointestinal system, especially in chronic or cumulative exposure. NPs particles that enter through the digestive system can be absorbed by the intestine and spread to various organs through the bloodstream. Their small size and hydrophobic surface allow NPs to penetrate the colonic mucosa, the innermost layer of the colon. To enter cells, NPs bind proteins during digestion, forming a protein corona that facilitates internalization (Jiang *et al.,* 2010; Walkey and Warren, 2012). The colonic mucosa, which is exposed to bacteria, food antigens, and toxic substances such as NPs, is the first layer to be affected. This layer consists of the epithelium, lamina propria, and muscularis mucosa (Eroschenko, 2012). In the lamina propria, densely packed crypts contain epithelial cells that play a role in mucus production and stem cells for tissue regeneration. Accumulation of NPs induces inflammation by increasing ROS production, which activates oxidative stress. This oxidative stress triggers the NF-κB signaling pathway, releasing pro-inflammatory cytokines that can lead to crypt epithelial cell death and crypt shortening. The submucosa, located between the mucosa and muscularis, is rich in immune cells and blood vessels. Exposure to NPs, especially at a dose of 4 µL NP/kg, resulted in significant submucosal edema. NPs cause vasodilation, increase endothelial permeability, and release inflammatory mediators such as cytokines and histamine. These mediators increase the leakage of fluid

and blood cells into the submucosal tissue, leading to oedema (Ismaya, 2017). The muscularis layer, which consists of smooth muscle, can be damaged by NPs exposure, triggering mitochondrial responses, ROS production, and oxidative stress. This long-term stress increases the release of inflammatory mediators that affect smooth muscle contractility and potentially cause hyperplasia or hypertrophy (Chen *et al.,* 2017). Thus, exposure to NPs at high doses can worsen the structure and function of colonic tissue, increase inflammation, and affect epithelial homeostasis, as well as worsen gastrointestinal tissue damage.

Microscopic observations of liver tissue of mice (Mus musculus) exposed to various doses of NPs showed significant and dose-responsive structural changes. In the control group (K), the liver tissue showed normal lobular architecture, with hepatocytes arranged radially around the central vein. The cell nucleus appeared round, the cytoplasm was homogeneous, and there were no vacuolization or degenerative signs (Figure 3). This normal liver structure is consistent with previous reports showing that hepatocytes are arranged trabecular pattern with intact cellular integrity and a moderate number of Kupffer cells (Guyton & Hall, 2019). However, in the treatment groups (P1–P3), there were significant morphological changes. Quantitatively (Table 2), the proportion of normal hepatocytes decreased drastically from 84.84 ± 1.20% in the control group to 47.85 ± 1.67% at the highest dose (P3). This decrease was accompanied by an increase in oedematous hepatocytes (from 2.97 ± 0.24% to 8.85 ± 1.38%) and necrosis (from 12.18 ± 1.22% to 43.31 ± 2.31%). Oedematous hepatocytes were characterized by cytoplasmic vacuolization and cell swelling, while necrotic cells showed nuclear pyknosis, karyorrhexis, and karyolitic, indicating a severe degenerative process (Singh *et al.,* 2019). The increase in the number of activated Kupffer cells was also significant, from 12.18 ± 1.23 to 104 ± 6.62 in the P3 group. Kupffer cells, which are liver macrophages, play a role in phagocytosis of foreign particles and the production of proinflammatory cytokines (such as IL-6 and TNF-α) in response to oxidative stress and inflammation (Park & Park 2019). The increase in the number of Kupffer cells reflects the activation of the innate immune system due to exposure to nanoparticles that cannot be phagocytosed efficiently (Fadeel & Garcia, 2010)

Figures 4 and 5 show significant dilation of the portal vein and central vein diameters. The portal vein diameter increased from 12.18 ± 1.24 µm to 132.44 ± 5.62 µm, while the central vein widened from 12.18 ± 1.25 µm to 76.64 ± 7.48 µm. This dilation is interpreted as a manifestation of vascular congestion and impaired intrahepatic blood flow that often occurs in acute inflammatory conditions or toxicant exposure (Reddy & Rao, 2006). A study by Lu *et al.* (2016) also showed that NPs can disrupt microvasculature homeostasis, activate vascular endothelium, increase permeability, and cause tissue oedema (Lu *et al.,* 2016)

The liver contains hepatocytes that make up about 60% of the organ parenchyma (Williams *et al.,* 2002). Normal hepatocytes maintain intact cell membranes and nuclei. Oedematous hepatocytes, which are swollen with fluid, are an indication of impending necrosis. Oedema is a sign of inflammation, a defensive response aimed at tissue repair (Silbernagl and Florian, 2013). Hepatocyte necrosis, which is characterized by the dissolution and shrinkage of cell membranes, causes cell death (Luedde *et al.,* 2014). In this study, the decrease in normal hepatocytes and the increase in necrotic hepatocytes with increasing NP exposure are in line with the findings of Sayed *et al.* (2024), who reported similar effects on tilapia liver due to exposure to plastic particles. The decrease in oedematous hepatocytes in the high-dose group coincided with an increase in necrotic hepatocytes, with higher NP exposure accelerating necrosis (Sayed et al, 2024). Kupffer cells play an important role in clearing toxins and pathogens from the liver. As the concentration of NPs increased, the number of Kupffer cells also increased, which correlated with a higher proportion of necrotic hepatocytes. This is consistent with Kolios' (2006) study, which showed that Kupffer cells are activated by necrotic hepatocytes, which contribute to the liver's immune response to infection or injury (Han and Ulevitch, 2005). The portal vein, which carries blood to the liver, has a larger diameter than the central vein that carries blood out. The smaller vein diameter in the 1 µL/kg group correlated with a higher proportion of oedematous hepatocytes, which pushed the vein lumen and reduced its size. In contrast, the larger diameters of the portal vein and central vein in the 2 µL and 4 µL/kg groups corresponded to increased necrosis, where smaller necrotic hepatocytes did not compress the surrounding blood vessels. These findings support the work of Masyuk *et al.* (2003), who noted that the portal vein, with its thin wall and low pressure, is more susceptible to expansion from the surrounding tissue (Masyuk *et al.,* 2003). Therefore, the NPs-induced inflammatory response appears to cause venous dilation as necrotic cells spread from the portal to the central vein area (Makiyah and Khumaisah, 2018). Overall, NPs exposure caused obvious

structural changes in the liver tissue of mice, which were dose-responsive. Increased numbers of edematous and necrotic hepatocytes, accompanied by increased Kupffer cell activation and blood vessel dilation, illustrate the damage mechanisms associated with inflammation and vascular disruption. These findings indicate the potential toxicity of NPs to the liver, which may disrupt organ function and increase the risk of further damage at high dose exposure.

The spleen, as a secondary lymphoid organ, has an important function in antigen filtration and adaptive immune response. Figure 6 and Table 3 show that NPs exposure also significantly affected the histological structure of the mouse spleen. In the control group, the white and red pulp structures were clearly visible, with compact periarteriolar lymphoid sheath (PALS) areas and germinal centres and well-defined boundaries. However, in the treatment group, there were progressive changes in the architecture of the lymphoid tissue, especially in the P3 group, which showed disorganization of the white pulp, enlargement of the germinal centre, and loss of the boundary between the white and red pulp (Figure 6d). The number of normal hepatocytes increased from 635.74 ± 5.93 to 1015.20 ± 6.18, which can be interpreted as the proliferation of immune cells, especially lymphocytes and macrophages. This increase often occurs in systemic inflammatory conditions or immune hyperactivation triggered by exposure to foreign particles (Barillet *et al.,* 2010). The increase in cell oedema (from 125.02 ± 3.51 to 222.07 ± 3.02) and necrosis (from 64.56 ± 3.13 to 86.77 ± 1.58) indicated oxidative stress and cell death due to intracellular redox imbalance, which has been reported as one of the main mechanisms of NPs toxicity in lymphoid tissues (Poma *et al.,* 2019).

The number of Kupffer-like cells in the spleen was also increased (from 55.48 ± 1.73 to 70.52 ± 2.11). Although typical Kupffer cells are found in the liver, the presence of tissue macrophages in the spleen showing similar morphology suggests increased phagocytic activity to eliminate cellular debris and foreign particles. This excessive activation may aggravate local inflammation and disrupt lymphoid tissue homeostasis (Sun *et al.,* 2022).

Nanoplastics can enter the body via the bloodstream and accumulate in the spleen, where they initiate an immune response. This process begins with oxidative stress caused by the formation of free radicals or ROS from NPs. Acting as antigen signals, NPs trigger an inflammatory response and increase the proliferation of immune cells. This reaction is regulated by signalling pathways, including nuclear factor-kappa B (NF-kB) and mitogen-activated protein kinase (MAPK), which control the production of inflammatory mediators. NF-kB, a key regulator of innate immunity, links cellular danger signals to antigen signals provided by NPs (Serhan *et al.,* 2010). The spleen plays a critical role in initiating immune responses, including responding to infections and removing antigens and cell debris from the blood (Mebius & Kraal, 2005; Bronte & Pittet, 2013).

The spleen consists of white pulp and red pulp, with this study focusing on the white pulp. The white pulp includes the marginal zone, germinal centres, and the periarteriolar lymphoid sheath (PALS), which is the T cell zone. The germinal centre is where B lymphocytes are generated, while the marginal zone contains various immune cells such as marginal zone B cells, macrophages, and dendritic cells. These B cells are able to respond rapidly to antigens by producing antibodies (Borges da Silva *et al.,* 2022). NP exposure causes an enlargement of the white pulp diameter, which is associated with the proliferation and differentiation of B cells and the expansion of germinal centres. This requires the involvement of CD4+ T cells, which are activated by dendritic cells that transport antigens to B cells, thus enhancing immune defence through antibody production. NP, which acts as an antigen signal, is specifically recognized by B and T cells, which trigger hyperplasia in the spleen. This results in an increase in the diameter of the white pulp and germinal centres. In addition, NP delivered to the PALS via antigen-presenting cells (APCs) is processed by T cells, activating them, and stimulating their proliferation and differentiation. This cytokine-driven response results in increased thickness of the PALS and marginal zone. CD4+ T cells in the PALS may also aid in the activation of B cells in the germinal center, where activated B cells differentiate into plasma cells that produce specific antibodies (Darwin *et al.,* 2021).

CONCLUSION

The variation in NPs concentrations significantly impacts the histological structure of the colon, liver, and spleen of rats. In the colon, this is evidenced by increased thickness in the submucosa and muscularis layers, as well as a reduction in crypt length. In the liver, variations in NPs concentration affect the percentage of normal and oedematous hepatocytes, with a notable increase in necrotizing hepatocytes, the number of Kupffer cells, and the diameter of both the portal and central veins. In the

spleen, the different concentrations of NPs lead to an enlargement of the white pulp and germinal center diameters, as well as increased thickness in PALS and the marginal zone.

ACKNOWLEDGEMENTS

Authors would like to thank the Directorate of Research, Technology, and Community, Ministry of Education, Culture, Research and Technology, Universitas Airlangga, Indonesia, for the funding via Master Thesis Research Activities in 2022 Grant no.1004/UN3/2022, May 11th 2022.

CONFLICT OF INTEREST

Authors declare that there is no conflict of interest regarding the publication of this article. The research was conducted independently without any financial or personal relationships that could influence the results and interpretations of this study.

REFERENCES

Barillet S, Simon-Deckers A, Herlin-Boime N, Mayne-L'Hermite M, Reynaud C, Cassio D, Gouget B and Carrière M, 2010. Toxicological consequences of TiO_2, SiC nanoparticles and multi-walled carbon nanotubes exposure in kidney cells. *Nanotoxicology* 4(4): 382–393.

Borges da Silva H, Fonseca R, Pereira RM, Cassado Ados A, Álvarez JM and D'Império Lima MR, 2015. Splenic macrophage subsets and their function during blood-borne infections. *Frontiers in Immunology 6*: 480.

Bronte V and Pittet MJ, 2013. The spleen in local and systemic regulation of immunity. *Immunity,* 39: 806–818.

Chen W, Lu C, Hirota C, Iacucci M, Ghosh S and Gui X, 2017. Smooth muscle hyperplasia/hypertrophy is the most prominent histological change in Crohn's fibrostenosing bowel strictures: A semiquantitative analysis by using a novel histological grading scheme. *Journal of Crohn's and Colitis* 11(1): 92–104.

Clarinsa RM and Sutoyo S, 2021. Pembuatan dan karakterisasi plastik biodegradable dari komposit HDPE (High Density Polyethylene) dan pati umbi suweg (Amorphophallus campanulatus). *UNESA Journal of Chemistry*, 10(1).

Darwin E, Elvira D and Elfi EF, 2021. *Imunologi dan infeksi.* Andalas University Press.

Eroschenko VP, 2012. *Atlas Histologi diFiore*. Jakarta: EGC.

Fadeel B and Garcia-Bennett AE, 2010. Better safe than sorry: understanding the toxicological properties of inorganic nanoparticles manufactured for biomedical applications. *Advanced Drug Delivery Reviews* 62(3): 362–374.

Giri S, Dutta P and Giri TK, 2021. Inulin-based carriers for colon drug targeting. *Journal of Drug Delivery Science and Technology*.

Guyton AC and Hall JE, 2016. *Textbook of Medical Physiology*. 13th ed. Philadelphia: Elsevier.

Han J and Ulevitch RJ, 2005. Limiting inflammatory responses during activation of innate immunity. *Nature Immunology* 6: 1198–1205.

Hayati A, Pramudya M, Soepriandono H, Astri AR, Kusuma MR, Maulidah S, Adriansyah W and Dewi FRP, 2022a. Assessing the recovery of steroid levels and gonadal histopathology of tilapia exposed to polystyrene particle pollution by supplementary feed. *Veterinary World* 15(36): 517–523.

Hayati A, Pramudya M, Soepriandono H, Wahyuni AD and Dewi FRP, 2022b. Effects of medicinal plants rhizome on growth performance of tilapia (Oreochromis niloticus) exposed to microplastics. *AIP Conference Proceedings* 2554: 090012.

Hayati A, Wilujeng WP, Pramudya M, Dewi FRP, Sugiharto B, Muchtaromah RJK and Susilo, 2024. The effect of exposure to polystyrene nanoplastics on cytokine levels and reproductive system of male tilapia. *Tropical Journal of Natural Product Research* 8(2):6300–6303.

Ismaya R, Rosmaidar and Nazaruddin, 2017. Pengaruh paparan timbal (Pb) terhadap histopatologi usus ikan nila (Oreochromis niloticus). *JIMVET* 2(1): 12–16.

Jiang X, Weise S, Hafner M, Rocker C, Zhang F and Wolfgang JP, 2010. Quantitative analysis of protein corona on FePt nanoparticles formed by transferrin binding. *Journal of the Royal Society Interface* 7: S5–S13.

Jin Y, Wu S, Zeng Z and Fu Z, 2022. Polystyrene nanoplastics exposure induces gut microbiota dysbiosis and intestinal inflammation in mice. *Journal of Hazardous Materials* 423: 127167.

Joksimovic N, Selakovic D, Jovicic N, Jankovic N, Pradeepkumar P, Eftekhari A and Rosic G, 2022. Nanoplastics as an invisible threat to humans and the environment. *Journal of Nanomaterials* 2022(1): 1–15.

Kibria G, Nahid I M, Rafat S, Huy QN and Monjur M, 2023. Plastic waste: challenges and opportunities to mitigate pollution and effective management, *International Journal of Environmental Research* 17(20).

Kolios G, Valatas V and Kouroumalis E, 2006. Role of Kupffer cells in the pathogenesis of liver disease. *World Journal of Gastroenterology* 12(46): 7413–7420.

Kwak JI and An YJ, 2021. Microplastic digestion generates fragmented nanoplastics in soils and damages earthworm spermatogenesis and coelomocyte viability. *Journal of Hazardous Materials*: 402.

Lewis SM, Williams A and Eisenbarth SC, 2019. Structure-function of the immune system in the spleen. *Science Immunology*, 4(33): eaau6085.

Lim JW, Kim HM, Lee SH, Park JH, Choi MJ, Lee HR, Kim DH and Lee HJ, 2021. Nanoplastics induce intestinal inflammation via TLR4-NFκB signaling pathway in mice. *Environmental Pollution* 274.

Lithner D, Larsson A and Dave G, 2011. Environmental and health hazard ranking and assessment of plastic polymers based on chemical composition. *Science of The Total Environment* 409: 3309–3324.

Liu L, Fokkink R and Koelmans AA, 2016. Absorption of polycyclic aromatic hydrocarbons to polystyrene nanoplastic. *Environmental Toxicology and Chemistry* 35: 1650–1655.

Lu Y, Zhang Y, Deng Y, Jiang W, Zhao Y, Geng J, Ding L and Ren H, 2016. Uptake and accumulation of polystyrene microplastics in zebrafish (*Danio rerio*) and toxic effects in liver. *Environmental Science and Technology* 50(7): 4054–4060.

Luedde T, Kaplowitz N and Schwabe RF, 2014. Cell death and cell death responses in liver disease: mechanisms and clinical relevance. *Gastroenterology* 147(4): 765-783.

Makiyah A dan Khumaisah LL, 2018. Studi gambaran histopatologi hepar tikus putih strain wistar YANG diinduksi aspirin pasca pemberian ekstrak etanol umbi iles-iles (*Amorphophallus variabilis* Bl) selama 7 hari. *Majalah Kedokteran Bandung* 50(2): 93–101.

Masyuk TV, Ritman EL and LaRusso NF, 2003. Hepatic artery and portal vein remodeling in rat liver. *American Journal of Pathology* 162(4): 1175–1182.

Mebius RE and Kraal G, 2005. Structure and function of the spleen. *Nature Reviews Immunology* 5: 606–616.

Park EJ and Park K, 2009. Oxidative stress and pro-inflammatory responses induced by silica nanoparticles in vivo and in vitro. *Toxicology Letters* 184(1): 18–25.

Phuong NN, Vergnoux AZ, Poirer L, Kamari A, Chatel A, Mouneyrac C and Lagarde F, 2016. Is there any consistency between the microplastics found in the field and those used in laboratory experiments? *Environmental Pollution* 211: 111–123.

Pizzino G, Irrera N, Cucinotta M, Pallio G, Mannino F, Arcoraci V, Squadrito F, Altavilla D and Bitto, A, 2017. Oxidative stress: harms and benefits for human health. *Oxidative Medicine and Cellular Longevity*: 1-13.

Poma A, Vecchiotti G, Colafarina S, Zarivi O, Aloisi M, Arrizza L, Chichiriccò G and Di Carlo P, 2019. In vitro genotoxicity of polystyrene nanoparticles on the human fibroblast Hs27 cell line. *Nanomaterials* 9(9): 1299.

Reddy JK and Rao MS, 2006. Lipid metabolism and liver inflammation. II. Fatty liver disease and fatty acid oxidation. *American Journal of Physiology-Gastrointestinal and Liver Physiology* 290(5): G852–G858.

Sayed AH, Walaa FAE, Karima AB, Zeinab A, Jae-Seong L and Salwa M, 2024, Polystyrene nanoplastic and engine oil synergistically intensify toxicity in Nile tilapia, Oreochromis niloticus, *BMC Veterinary Research*, 20, 143.

Serhan CN, Ward PA and Gilroy DW, 2010. *Fundamentals of inflammation*. New York: Cambridge University Press.

Silbernagl S dan Lang F, 2013. *Teks dan Atlas Berwarna Patofisiologi*. Jakarta: EGC.

Singh N, Manshian B, Jenkins GJ, Griffiths SM, Williams PM, Maffeis TG, Wright CJ and Doak SH, 2009. Nanogenotoxicology: the DNA-damaging potential of engineered nanomaterials. *Biomaterials*, 30(23): 3891–3914.

Soepriandono H, Pramudya M, Nurbani FA, Dewi FRP, Vuanghao L, Muchtaromah B and Hayati A, 2025. Protection of exogenous antioxidant of *Cinnamomum burmanii* as a hepatoprotective on the toxicological responses of nanoplastics in rats (*Rattus norvegicus* L.). *Research Journal of Pharmacy and Technology* 18(1): 365-371.

Sun X, Chen B, Li Q, Liu N, Xie Y, Zhao Y, Zhang Y, Wang B and Li R, 2022. Immunotoxicity of micro- and nanoplastics: A review of recent studies on immune responses. *Science of the Total Environment* 832: 155041.

Tankovic MS, Perusco S, Gordrijan VJ and Pfannkuchen M, 2015. Marine plastic debris in the northeastern adriatic. *Proceedings of the MICRO 2015 Seminar of Microplastic Issues*.

Triwahyudi H, Soehargo L, Muniroh L, Qolbi RN, Aini TQ, Kurnia RF, Putra PA, Pramudya M, Muchtaromah B and Hayati A, 2023. Potential of red seaweed (*Dichotoma obtusata*) on immune response and histopathology of rat testis exposed to nanoplastics. *Tropical Journal of Natural Product Research* 7(5): 2969-2973.

Walkey C and Warren CWC, 2011. Understanding and controlling the interaction of nanomaterials with proteins in a physiological environment. *Chemical Society Reviews* 41(7): 2780–2799

Williams GM and Latropoulos MJ, 2002. Alteration of liver cell function and proliferation: differentiation between adaptation and toxicity. *Toxicologic Pathology*, 30(1): 41–53.

Wu B, Wu X, Liu S, Wang Z and Chen L, 2019. Effects of polystyrene microplastics on the gut barrier, microbiota and inflammatory response in mice. *Science of the Total Environment* 708: 134594.

Yin J, Ju Y, Qian H, Wang J and Miao X, 2022. Nanoplastics and microplastics may be damaging our livers. *Toxics* 10(10): 586.

Yong CQY, Valiyaveettil S and Tang BL, 2020. Toxicity of microplastics and nanoplastics in mammalian systems. *International Journal of Environmental Research and Public Health* 17(5): 1509.